C. R. Mecanique 339 (2011) 42–57

Contents lists available at ScienceDirect

Comptes Rendus Mecanique

www.sciencedirect.com

Laminar free convection in undulated cavity with non-uniform boundary conditions

Amina Sabeur-Bendehina *, O. Imine, L. Adjlout

Department of Marine Engineering, Mechanical Engineering Faculty, BP 1505, El M'Naouer, USTO University, Oran, Algeria

ARTICLE INFO

Article history:
Received 26 August 2010
Accepted after revision 17 November 2010
Available online 7 January 2011

Keywords:
Heat transfer
Natural convection
Wavy hot wall
Non-uniform boundary conditions
Aspect ratio
Wavelength

ABSTRACT

In the present work, the influence of non-uniform boundary conditions on natural convection in inclined rectangular cavities differentially heated is studied. The hot wall is wavy with three undulations. The aspect ratio of the cavities has also been changed. Various inclination angles were performed. The flow and the heat transfer are calculated by solving both Navier–Stokes and the energy equations with finite volume method in the primitive formulation.

The sinusoidal distribution of temperature is imposed at the vertical walls and was compared with isothermal boundary conditions. The flow and the heat transfer are also simulated for different wavelength of the sinusoidal distribution. It was found that this parameter has an effect on the trend of the local Nusselt number.

The results obtained show that the trend of the local Nusselt number is wavy for all inclination angles and for all the configurations tested. The mean Nusselt number decreases comparing with the Nusselt number of the square cavity. Non-uniform boundary conditions of the temperature distribution in both vertical walls increase the local and the mean Nusselt number comparing with the isotherm walls. The sinusoidal distribution seems to reduce the heat transfer rate for two wavelengths and increasing aspect ratio results in a decrease of the Nusselt number.

1. Introduction

Natural convection in enclosures has been extensively studied both experimentally and numerically in recent years being of considerable interest in many engineering and science applications such as boilers, nuclear reactor systems, energy storage and conservation, fire control, chemical food and metallurgical industries.

Most of papers in this field are substantially orientated toward the study of rectangular enclosures as by De Vahl Davis [1], Catton [2], Ostrach [3], Yang [4] and Bejan [5]. They have shown the importance of the inclination on its performance. A more comprehension of the flow behaviour and the heat transfer in such cavities was needed. The study of aspect ratio and inclination angle influence has allowed the understanding of the heat transfer behaviour by Arnold [6], Ozoe [7], Hollands and Raithby [8] and Kuyper et al. [9]. Using the vorticity–stream function approach, Wilkes and Churchill [10] applied the ADI method and obtained 2D fluid flow distribution inside the cavity for aspect ratios ranging from 1 to 3.

Chu and Churchill [11] used the latter method to describe the solution of heat transfer in a cavity with aspect ratios ranging from 0.4 to 5 and Rayleigh number up to 5×10^4. Korpela and Lee [12] presented also natural convection heat

* Corresponding author.
E-mail address: asabeur@univ-usto.dz (A. Sabeur-Bendehina).

1631-0721/$ – see front matter
doi:10.1016/j.crme.2010.11.001

Nomenclature

A	Aspect ratio of the cavity $A = \frac{L}{H}$
a	Thermal diffusivity
C_p	Specific heat
g	Gravitational acceleration
H	Width of the cavity
k	Wavelength of the temperature distribution
L	Length of the cavity
Nu	Nusselt number
P	Pressure
Pr	Prandtl number $Pr = \frac{\nu}{\alpha'}$
Ra	Rayleigh number $Ra = \frac{g\beta(T_h - T_c)H^3}{\nu\alpha'}$
T	Temperature
u_1, u_2	Dimensionless velocity components
x, y	Dimensionless Cartesian coordinates

Greek symbols

α	Coefficient of temperature distribution
α'	Thermal diffusivity
β	Thermal expansion coefficient
ΔT	Temperature difference, $[T_h - T_c]$
ϕ	Inclination angle
ν	Cinematic viscosity
ψ	Maximum value of the stream function
ρ	Density of fluid
θ	Dimensionless temperature
ξ, η	Dimensionless curvilinear coordinates
ϑ	General variable representing u, v and θ

Subscripts

$\overline{Nu}$	Average Nusselt number
c, h	Cold and hot walls
L	Local
Max, Min	Maximum and minimum values
ξ, η	Derivative relative to ξ, η respectively

transfer in rectangular cavities; they investigated the cavities with aspect ratios up to 40 by determining the boundary between various flow regimes occurring in cavities with rather high aspect ratios.

Yao [13] has studied theoretically the natural convection along a vertical wavy surface. He found the heat transfer rate for a wavy surface smaller than of corresponding flat plate case and decreases with increase of the wave amplitude. The average Nusselt number also shows the same trend. Saidi et al. [14] also presented numerical and experimental results of the flow over and heat transfer from a sinusoidal cavity. They reported that the total heat exchange between the wavy wall of the cavity and the following fluid was reduced by the presence of vortex. Adjlout et al. [15] studied the natural convection in an inclined cavity with hot wavy wall; they simulated the heat transfer and the fluid flow with ADI scheme. One of their interesting results was the decrease of average heat transfer with the surface waviness compared with a square cavity. Belkadi et al. [16] treated the same geometry of the cavity but they added partial partitions on the hot wall; they found in their study that the mean Nusselt number decreases notably compared with the heat transfer in the square undulated cavity without partitions. The usual situations analysed refer to enclosures with imposed uniform temperature at the vertical walls. Gilly et al. [17] have shown the importance of the non-uniform distribution of the temperature on the hot wall, a more comprehension of the flow behaviour and the heat transfer with such boundary conditions was required. They proposed an application of their work in solar collectors: the absorber which collects the incidental solar radiation and the cover generally out of glass, which reduces the losses by radiation and convection of the absorber. The studies devoted to this type of problem are generally placed in the case or these two active surfaces are isothermal whereas in the majority of the practical problems, the temperatures are not constant. For the solar collector, the circuit of recovery which consists of a network of tubes plated against the absorber and traversed by a coolant induces a variation in temperature along the absorber. These variations in temperature on the active walls were simulated by a sinusoidal law. This kind of heating is found also in glass technology and in crop drying applications such as corn and rice (Bassey and Schmidt [18]).

The effect of non-uniform temperature distribution on an inclined three-dimensional enclosure has been studied by Chao et al. [19]. Bottom wall is maintained at a saw-toothed temperature distribution with different amplitude and orientation while top wall is isothermal and other faces are adiabatic. The circulation pattern did not change significantly with the temperature distributions. The convective motion in a square cavity with linearly varying temperature imposed along the top surface has also been investigated numerically by Shukla et al. [20]. Jian Li et al. [21] have treated the problem of the natural convection on vertical flat plate with a sinusoidal temperature distribution.

In the present paper, a numerical investigation of the influence of boundary conditions on free convection in an inclined square and rectangular cavities with wavy wall, differentially heated has been performed. The aspect ratio of the cavities has also been changed. The hot wall is wavy; the two vertical walls are heated with sinusoidally varying temperature distribution as proposed by Gilly et al. [17] with different wavelengths. The study has been conducted at different inclination of the enclosure while Rayleigh number was fixed to 10^5.

2. Problem specification

The problem treated is a two-dimensional heat transfer in a square and rectangular cavity. The vertical walls are heated with non-uniform distribution of dimensionless temperature defined as follow (Fig. 1):

$$\theta_h(1, y) = \frac{1}{2} + \alpha \operatorname{Sin}\left(2k\pi\left(\frac{y}{A} - \frac{1}{2}\right)\right)$$

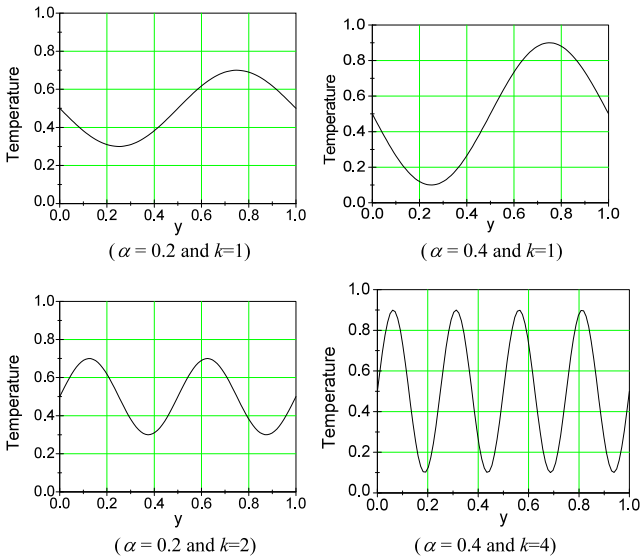

Fig. 1. Sinusoidal distribution of the temperature.

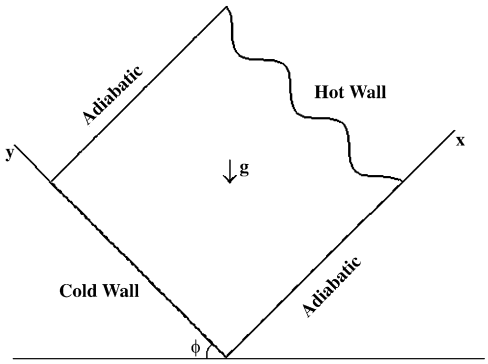

Fig. 2. Geometry of the cavity.

$$\theta_c(0, y) = -\frac{1}{2} + \alpha \operatorname{Sin}\left(2k\pi\left(\frac{y}{A} - \frac{1}{2}\right)\right)$$

k is the temperature distribution wavelength. The coefficient α determines the maximum rate of variation compared to the average temperature along the wall. It varies between 0 and 0.4 in the present study.

The shape of the wavy vertical hot wall is taken as sinusoidal. The expression of the wavy wall is given by:

$$f(y) = \left[1 - \text{Amp}(1 - \cos 2\pi n y)\right]$$

n and Amp are the number of undulations and the amplitude respectively (Fig. 2).

3. Analysis

Natural convection is governed by the differential equations expressing the conservation of mass, momentum and energy. The present flow is considered steady, laminar, incompressible and two-dimensional. The viscous dissipation term in the energy equation is neglected. The momentum equations are simplified using Boussinesq approximations, in which all fluid properties are assumed constant except the density in its contribution to the buoyancy force.

The influence of the ratio A is essential in this study knowing the importance of this parameter. In the rectangular configurations, the latter has been introduced in dimensionless form and the results are presented function of this ratio. The governing equations are given using the following dimensionless variables:

$$x = \frac{x^*}{H}, \qquad y = \frac{y^*}{L}$$

$$u_1 = \frac{u_1^*}{\nu/H}, \qquad u_2 = \frac{u_2^*}{\nu/L}$$

$$p = \frac{p^* H^2}{\rho \alpha'^2}, \qquad \theta = \frac{(T - T_0)}{T_h - T_c}$$

with

$$T_0 = (T_h + T_c)/2$$
$$\Delta T = T_h - T_c$$

Continuity equation:

$$\frac{\partial u_1}{\partial x} + \frac{1}{A^2}\frac{\partial u_2}{\partial y} = 0$$

Momentum equations:

$$u_1 \frac{\partial u_1}{\partial x} + \frac{1}{A^2} u_2 \frac{\partial u_1}{\partial y} = -\frac{1}{Pr^2}\frac{\partial P}{\partial x} + \left(\frac{\partial^2 u_1}{\partial x^2} + \frac{1}{A^2}\frac{\partial^2 u_1}{\partial^2 y}\right) + \frac{Ra}{Pr}\theta \,\mathrm{Cos}(\phi)$$
$$u_1 \frac{\partial u_2}{\partial x} + \frac{1}{A^2} u_2 \frac{\partial u_2}{\partial y} = -\frac{1}{Pr^2}\frac{\partial P}{\partial y} + \left(\frac{\partial^2 u_2}{\partial x^2} + \frac{1}{A^2}\frac{\partial^2 u_2}{\partial^2 y}\right) + A\frac{Ra}{Pr}\theta \,\mathrm{Sin}(\phi)$$

Energy equation:

$$u_1 \frac{\partial \theta}{\partial x} + \frac{1}{A^2} u_2 \frac{\partial \theta}{\partial y} = \frac{1}{Pr}\left(\frac{\partial^2 \theta}{\partial x^2} + \frac{1}{A^2}\frac{\partial^2 \theta}{\partial y^2}\right)$$

ϕ is the inclination angle of the enclosure.

The no-slip boundary conditions $u_1 = u_2 = 0$ are then imposed at the four walls of the cavity. The heat transfer rate by convection in an enclosure is obtained from the Nusselt number calculation. On the wavy wall, the local and the mean Nusselt numbers are expressed respectively:

$$Nu_L = \frac{\partial \theta}{\partial n}$$
$$\overline{Nu} = \frac{1}{s}\int_0^s \frac{\partial \theta}{\partial n}\,\mathrm{d}s$$

4. Square cavity

4.1. Grid validation

A grid independency study is performed for the square cavity by using equidistant grids of size 40×40, 50×50, 67×67 and 83×83. Table 1 shows the computed minimum, maximum and average Nusselt numbers throughout the cavity, the maximum horizontal and vertical velocity components, and the maximum stream function magnitudes as well as their position of occurrence results of De Vahl Davis [1] are also shown in the table. It is clearly seen that the agreement is excellent with the deviation of less than 1%. So the grid 67×67 (Fig. 3) is chosen for further computations.

Table 1
Validation of the grid.

	40×40	50×50	67×67	83×83	De Vahl Davis [1]
$\lvert\Psi_{\mathrm{Max}}\rvert$	9.631	9.633	9.617	9.632	9.612
X	0.285	0.285	0.285	0.285	0.285
Y	0.600	0.600	0.600	0.600	0.600
$u_{1\,\mathrm{Max}}$	34.623	34.721	34.699	34.661	34.730
Y	0.855	0.855	0.855	0.855	0.855
$u_{2\,\mathrm{Max}}$	68.82	68.66	68.591	68.88	68.59
X	0.065	0.065	0.065	0.065	0.065
$\overline{Nu}$	4.48	4.52	4.518	4.537	4.519
Nu_{Max}	7.70	7.77	7.711	7.78	7.717
Nu_{Min}	0.715	0.685	0.728	0.705	0.729

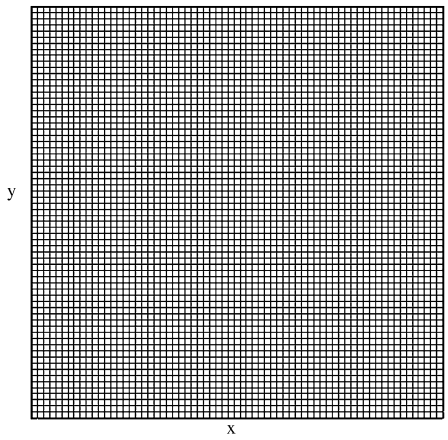

Fig. 3. Mesh distribution in the square cavity.

4.2. Numerical procedure

The equations governing the flow and the energy are solved using a finite volume method with pressure-correction method as introduced by Patankar [22]. After each line, Gauss Seidel sweep for the momentum, energy and the Poisson equation for the pressure correction were solved directly over the full domain. For the pressure correction, a second order scheme is used with 0.3 under relaxation factor, while the second order upwind scheme is adopted for the momentum and the energy equations with the same value of under relaxation factor 0.7 (see Versteeg and Malalasekera [23]).

4.3. Results

Fig. 4 shows the isotherms and the streamlines inside the square cavity for various wavelengths, and various values of α. The isotherms are affected by this new distribution; however a clear intersection of the lines with the vertical walls thus causing cells which decrease in size when k increases. The number of these cells is equal to the number of undulations of the thermal distribution. On the walls of heat exchange, i.e. vertical walls; the thermal boundary layer narrows upwards by alternation; this alternation repeats as many time as the number of undulations of the temperature distribution. The streamlines show a flow pattern mainly mono cellular on which small cells in the central part of the cavity are superimposed. Their centres show an oblique direction whatever the value of k. When α passes from 0.2 to 0.4, the flow slows down because the maximum value of ψ decreases, this is indicated in Table 2. On the other hand the velocity of the cells increases when k varies periodically between the even and odd values thus causing the separation of the central cell in two cells.

The trend of local Nusselt number corresponds to the undulation of the temperature which has a sinusoidal form; the number of undulations in the graph of local Nusselt number corresponds to the number of undulations of the temperature (see Figs. 5 and 6).

Another remark can be made concerning Table 3 is that the heat transfer is increased for the odd wavelengths towards the growing direction of the value of α while for the even values, a light reduction of 2.6% for $k = 2$, 1.3% for $k = 4$ and 3.7% for $k = 6$.

5. Square cavity with wavy wall

5.1. Validation of the grid

The governing equations transformed from the system (x, y) to the boundary fitted coordinate system (ξ, η) are given by Amaresh [24]. Numerical grid generation becomes an important tool for use in the numerical solution of partial differential equations on arbitrarily shaped regions. The coordinate transformation technique advanced by Thomson [25] is used for the solution of problems over complex geometries.

In order to study the precision of calculations; various grids were tested. Table 4 shows the various grids used for the Rayleigh number equal to 10^5. The values of vertical and horizontal velocity, the number of average Nusselt number and the maximum value of the stream function are also presented. The choice of the grid 67×80 (Fig. 7) which is used in the rest of the study is justified by the fact that the difference between the found values is lower than 4%.

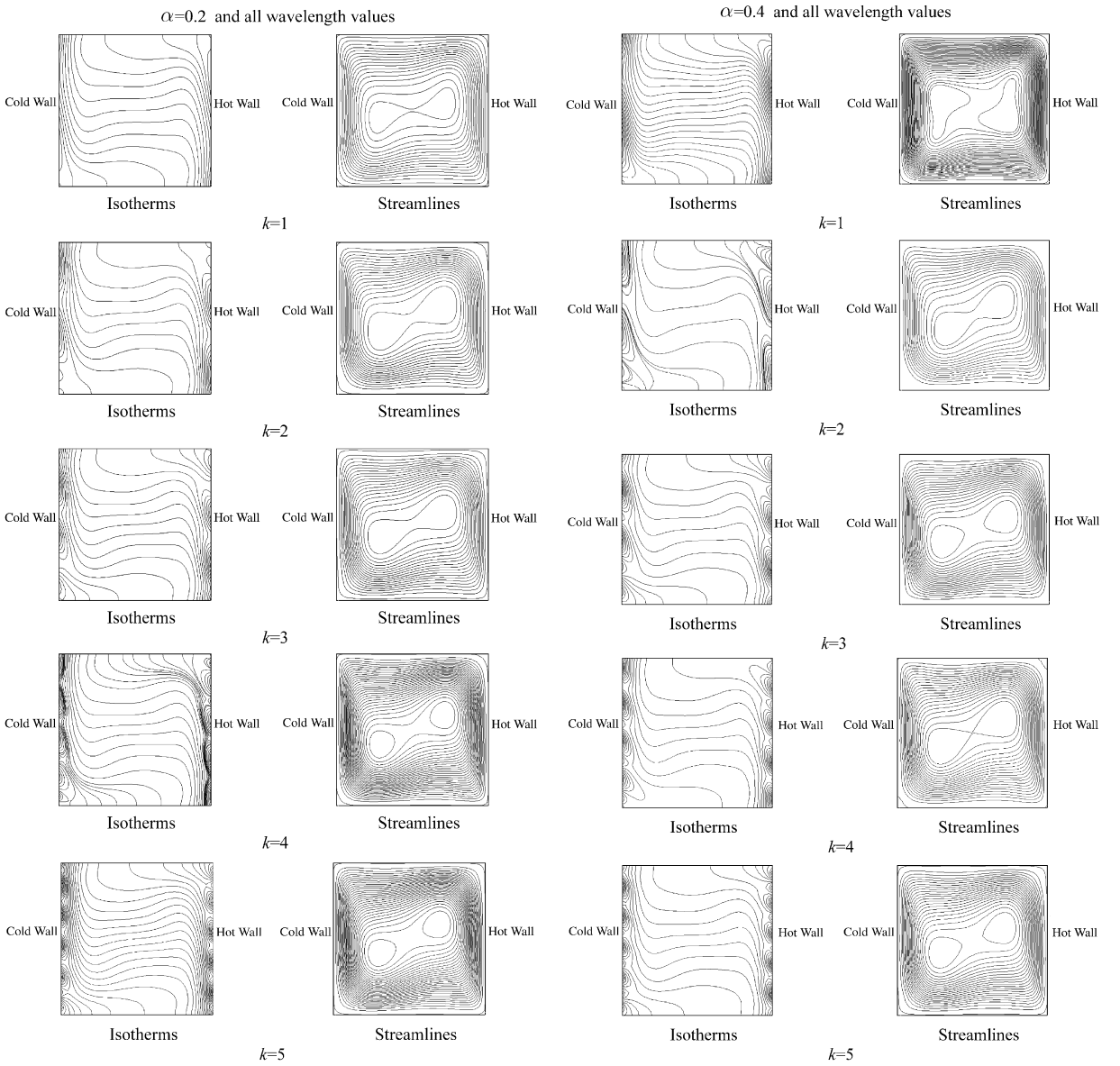

Fig. 4. Isotherms and streamlines for various values of k and α.

Table 2
Values of the ψ_{Max} for the sinusoidal distribution.

k	1	2	3	4	5
($\alpha = 0.2$)	8.06	9.76	9.63	9.68	9.65
X	0.75	0.71	0.76	0.73	0.74
Y	0.62	0.57	0.59	0.64	0.62
($\alpha = 0.4$)	7.46	10.05	9.44	9.73	9.61
X	0.73	0.69	0.70	0.71	0.68
Y	0.42	0.603	0.59	0.62	0.59

ψ_{Max} ($\alpha = 0$) = 9.61

5.2. Results

The sinusoidal distribution already met in the preceding section is imposed on the hot and cold vertical walls. Visualisations of the isotherms and the streamlines are presented in Fig. 8 for only one wavelength, $\alpha = 0.2$ and different angles.

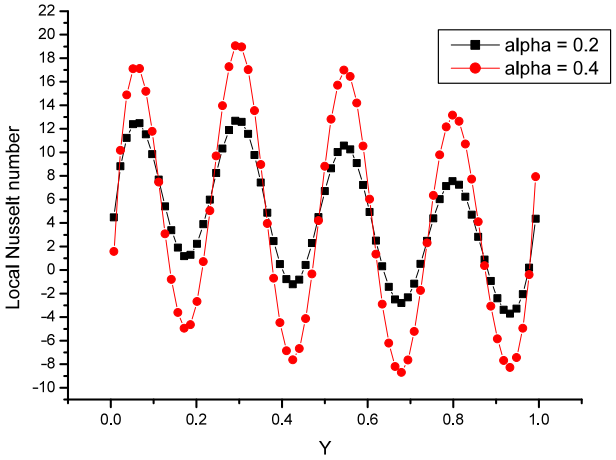

Fig. 5. Variation of local Nusselt number for $k = 4$ and different value of α.

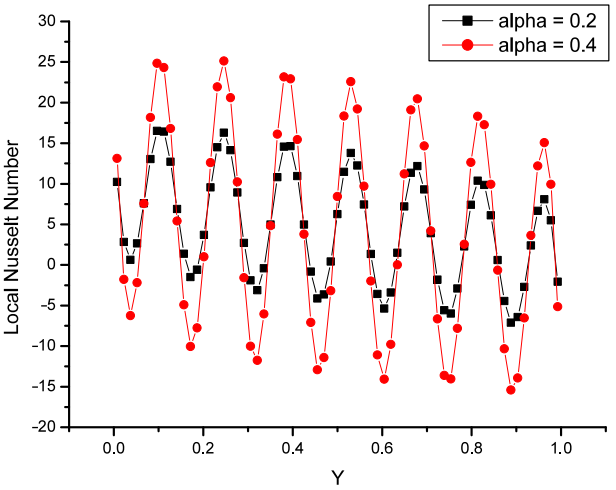

Fig. 6. Variation of local Nusselt number for $k = 7$ and different value of α.

Table 3
Value of the average Nusselt number for various values of α and k ($Ra = 10^5$).

k	1	2	3	4	5	6
$\overline{Nu}$ ($\alpha = 0.2$)	4.893	4.447	4.653	4.463	4.675	4.533
$\overline{Nu}$ ($\alpha = 0.4$)	5.18	4.331	4.745	4.402	4.723	4.362
$\overline{Nu}$ ($\alpha = 0$) = 4.518						

Table 4
Comparative table of the results (validation of the grid).

Grid	29×34	40×48	67×80	83×100
$\overline{Nu}$	3.907	3.82	3.760	3.72
ψ_{Max}	9.58	9.67	9.85	9.93
X	0.63	0.63	0.63	0.63
Y	0.60	0.60	0.60	0.60
U_{Max}	42.18	42.38	44.53	44.87
V_{Max}	66.06	66.99	68.61	68.96

For $\phi = 30°$, the fluid motion of the cells crossed inside the cavity. A small cell appears in the first top of the undulation. The thermo-convective flow involves a deviation of the isotherms. The non-uniform distribution affects seriously isotherms thus causing their intersections with the vertical walls. The thermal boundary layer is thin at the higher part of the undulation thus the heat transfer is with its maximum value. This tightening disappears just in the hollow from the undulation. This periodicity is due to the sinusoidal aspect of the temperature distribution and the geometrical shape of the hot wall. When $\phi = 60°$, the flow is accelerated in the higher corner of the cavity involving a small cell. The thermal boundary layer thickness increases in the hollow of the undulations and decreases at the tops. As for the central part of the cavity, a stratification of the isotherms is well established. For $\phi = 90°$, the gravitation is perpendicular to the adiabatic walls, Fig. 8 shows the acceleration of the flow within the cavity. It appears several separations in particular with the four corners of the cavity. The apparent cell is located at the higher corner of the cavity. The isotherms are also influenced by the non-uniform distribution. The tightening of the thermal boundary layer is done at the higher part of the undulation. This corresponds to minimal values of the local Nusselt number. For the angle $\phi = 120°$ and $150°$, the flow is mono-cellular in the heart of the cavity. The separation of the stream traces involves also the appearance of a cell in the higher corner of the cavity. The isotherms are increasingly dense in the vicinity of the corrugated wall.

5.3. Variation of the sinusoidal distribution wavelength

Fig. 9 shows the isotherms and the streamlines inside the cavity for various wavelengths and for $\alpha = 0.2$. The isotherms are again affected by the temperature distribution, in particular it exists an intersection of the lines with the vertical walls thus forming cells which decrease in size when k increases. The number of these cells is equal to the number of undulations of the sinusoidal function of the temperature imposed on the active walls. The isotherms are tighter in the lower part of the cavity on the hot wall. The increasing thermal boundary layer thickness was observed at the top of the undulation on the other hand a reduction with the hollow of the undulations of the hot wall. The cells formed along the corrugated wall involve extremums in the curve of local Nusselt for all the values of α studied (Figs. 10 and 11).

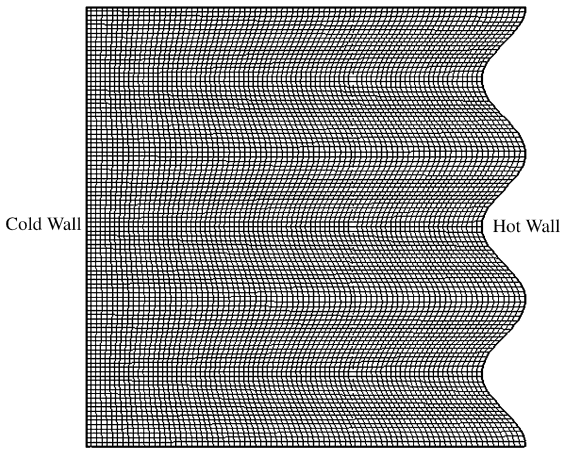

Fig. 7. Mesh distribution in the undulated cavity.

With regard to the streamlines; the direction of the cells is preserved for all the studied cases. When α passes from 0.2 to 0.4 a reduction in the volumetric flow is noticed for the wavelength values of the temperature distribution. Except for $k = 2$, it was observed an increase in the maximum value of ψ (Table 5). In the vicinity of the undulated wall, the velocity of the cells increases causing the appearance of several cells of size narrowed with the higher corner of the cavity.

Table 6 presents the maximum value of the stream function for all the values α and for all the studied wavelengths. The position in (X, Y) of each function is also given. It was noted that the position of the maximum value of ψ is roughly identical for the whole of the studied cases.

The trend of the local Nusselt number curve corresponds to the undulation of the temperature which has a sinusoidal form. The geometry of the hot wall does not influence the shape of the curve of local Nusselt number when k exceeds 1. Indeed, the trend of the local Nusselt number follows the undulation of the temperature distribution (Figs. 11 and 12). In addition, the geometry of the hot wall affects the average value of the Nusselt number (Table 7). It was recorded a reduction of 20% compared to the square cavity and an increase in:

- 6% for the passage from α 0 to 0.2,
- 7% for the passage from α 0.2 to 0.4.

6. Rectangular enclosures with wavy wall

The part of this paper is related to the rectangular cavities with undulated hot wall. In the present investigation, the tests were performed for the aspect ratios namely 3, 5, 7, 12 and 15.

The amplitude of the undulation for the aspect ratio 3 is fixed at 0.05 while the amplitude is fixed at 0.15 for the aspect ratios ranging from 5 to 15.

6.1. Transformation of the governing equations

By introducing the two new coordinates (ξ, η) in equation of continuity, momentum and energy respectively, the final forms of governing equations are:

- Continuity equation:

$$U_\xi + \frac{1}{A^2} V_\eta = 0$$

- Generalised momentum and energy equations:

$$(U\vartheta)_\xi + (V\vartheta)_\eta = S(\xi,\eta) + \left\{ \frac{\Gamma}{J}\left(\alpha\vartheta_\xi - \frac{\beta}{A^2}\vartheta_\eta\right)\right\}_\xi + \left\{ \frac{\Gamma}{J}\left(-\beta\vartheta_\xi + \frac{\gamma}{A^2}\vartheta_\eta\right)\right\}_\eta$$

where $\Gamma = 1$ for the momentum equation and $\Gamma = \frac{1}{Pr}$ for the energy equation. The source term $S(\xi, \eta)$ is given by:

$$S(\xi,\eta) = -y_\eta p_\xi - \frac{1}{Pr^2} y_\xi p_\eta \quad \text{for } \vartheta = u_1$$

$$S(\xi,\eta) = x_\eta p_\xi - \frac{1}{Pr^2} x_\xi p_\eta + JA\frac{Ra}{Pr}\theta \quad \text{for } \vartheta = u_2$$

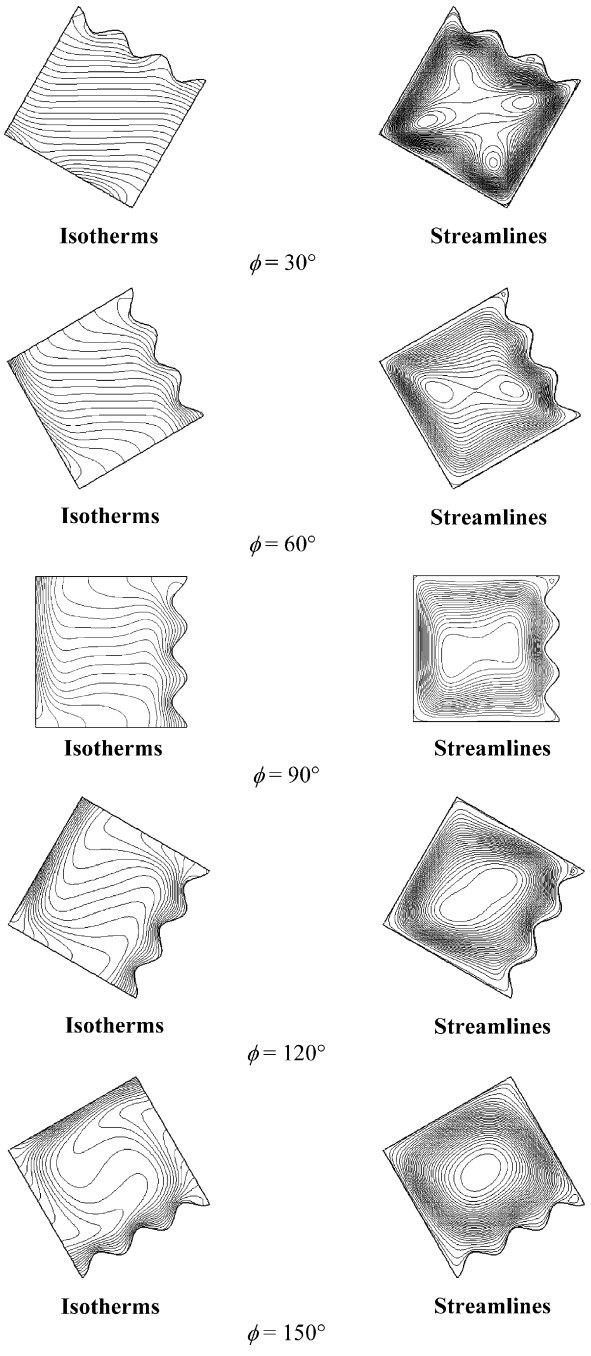

Fig. 8. Isotherms and streamlines for various inclination angles.

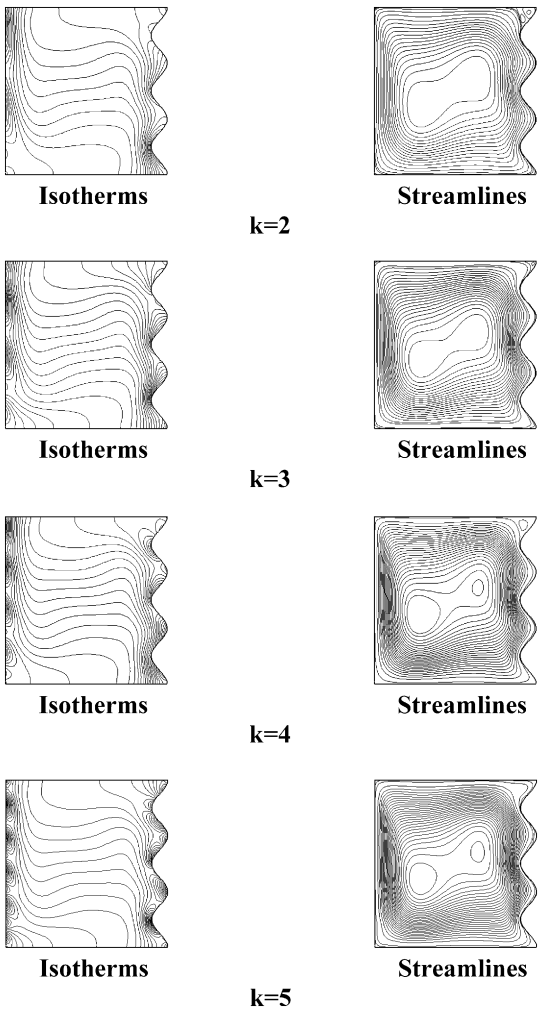

Fig. 9. Isotherms and streamlines of the square cavity with wavy hot wall and for $\alpha = 0.2$.

$$S(\xi, \eta) = 0 \quad \text{for } \vartheta = \theta$$

The relationships between the Cartesian and contravariant velocity components are:

$$U = y_\eta u_1 - x_\eta u_2$$

$$V = x_\xi u_2 - y_\xi u_1$$

where the geometric coefficients α, β, γ and the Jacobian J are given by:

$$\alpha = y_\eta^2 + x_\eta^2, \qquad \beta = x_\xi x_\eta + y_\xi y_\eta, \qquad \gamma = y_\xi^2 + x_\xi^2, \qquad J = x_\xi y_\eta - y_\xi x_\eta$$

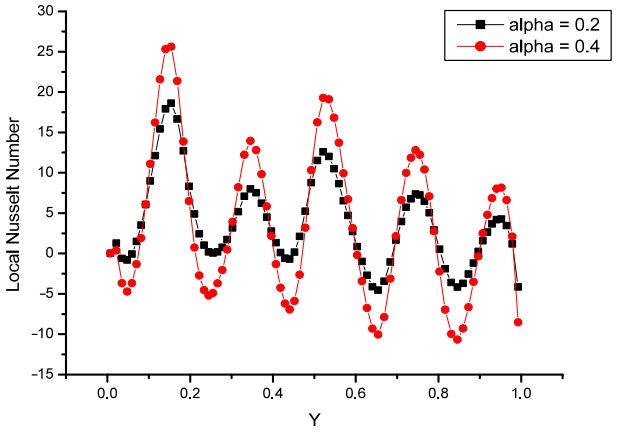

Fig. 10. Variation of the local Nusselt number along the hot wall ($k = 5$).

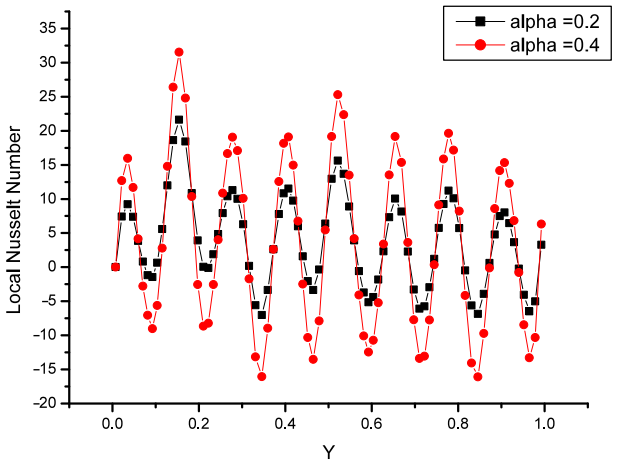

Fig. 11. Variation of the local Nusselt number along the hot wall ($k = 8$).

Table 5
Maximum values of the stream function for the sinusoidal distribution and various inclination angles.

ϕ	30°	60°	90°	120°	150°
ψ_{Max}	1.057	3.846	7.789	12.67	19.81
X	0.54	0.54	0.65	0.55	0.44
Y	0.69	0.60	0.52	0.68	0.52

Table 6
Maximum value of the stream function for all the values of α and k.

k	1	2	3	4	5
ψ_{Max} ($\alpha = 0.2$)	7.78	9.812	9.47	9.258	9.39
X	0.65	0.62	0.64	0.65	0.67
Y	0.52	0.57	0.59	0.57	0.51
ψ_{Max} ($\alpha = 0.4$)	6.23	10.394	9.28	9.23	9.35
X	0.62	0.58	0.63	0.66	0.63
Y	0.47	0.59	0.56	0.58	0.55
		ψ_{Max} ($\alpha = 0$) = 9.854			
		ψ_{Max} (square) = 9.61			

Table 7
Variation of the average Nusselt number for all the values of α and k.

k	1	2	3	4	5	6
$\overline{Nu}$ ($\alpha = 0.2$)	4.008	3.624	3.748	3.821	3.682	3.766
$\overline{Nu}$ ($\alpha = 0.4$)	4.295	3.509	3.777	3.918	3.732	3.784
			$\overline{Nu}$ ($\alpha = 0$) = 3.781			
			$\overline{Nu}$ (square) = 4.529			

Several grids have been tested for the different cavities. Table 8 shows the average Nusselt number for all the grids used, $Ra = 10^5$ and $\varphi = 90°$. Grid refinement was applied to check the accuracy of the solution. The number of grid cells used in the calculations was chosen such that the variation of the mean Nusselt number is less than 5%.

The final grids studied for different cavities are presented in Table 9.

6.2. Sinusoidal distribution on the vertical walls

In this part, only the streamlines and the isotherms for $A = 5$ are presented. The study was carried out in this paragraph for:

- $\alpha = 0.2$,
- $k = 1$.

Table 8
Validation of the grid for various cavities.

Grid ($A = 3$)	25×90	30×108	40×143	60×215
$\overline{Nu}$	3.46	3.44	3.47	3.50
Grid ($A = 5$)	25×135	30×162	40×215	60×324
$\overline{Nu}$	3.41	3.40	3.44	3.46
Grid ($A = 7$)	25×182	30×218	40×291	60×436
$\overline{Nu}$	3.39	3.36	3.35	3.37
Grid ($A = 12$)	25×304	30×365	40×487	60×730
$\overline{Nu}$	2.89	2.99	2.94	2.96
Grid ($A = 15$)	25×378	30×454	40×605	60×907
$\overline{Nu}$	2.79	2.75	2.77	2.80

Table 9
Final grids.

A	3	5	7	12	15
Grid	40×143	40×215	40×291	40×487	40×605

Table 10
Maximum values of the stream function for the sinusoidal distribution and various inclination angles.

ϕ	30°	60°	90°	120°	150°
ψ_{Max}	8.17	14.40	18.77	20.14	22.88
X	0.36	0.39	0.40	0.44	0.40
Y	1.66	1.84	1.84	1.99	2.13

Table 11
Variation of the average Nusselt number for all inclination angles.

ϕ	30°	60°	90°	120°	150°
$\overline{Nu}$	2.09	3.241	3.69	3.80	3.52

Fig. 12 presents the streamlines and isotherms for different inclination angles. For $\phi = 30°$, the fluid motion involves two cells in the central part of the cavity. The thermo convective motion gives deviation of the isotherms. In the vicinity of the vertical walls, the non-uniform distribution affects the isotherms thus forming intersection with the vertical walls. For $\phi = 60°$, the two cells are preserved with a light lengthening; this is with an acceleration of the flow. A thin thermal boundary layer appears at the three tops of the undulation; which causes an increase in the local Nusselt number.

For $\phi = 90°$, the gravitation is perpendicular to the adiabatic walls. The fluid motion is represented by a cell lengthened in the vertical direction of the cavity. The isotherms are influenced by the sinusoidal distribution of the temperature. Indeed, the intersection of the isotherms with the vertical walls was observed. The thickness of thermal boundary layer is highlighted in the undulations. This involves an increase in the local Nusselt number. Table 10 shows the maximum values of the stream function and their position in (X, Y). The flow grows simultaneously with the increase in the inclination angle giving appearance of cells for ϕ equal 120° and 150°.

The heat transfer, represented by the average Nusselt number, reaches a maximum for ϕ equal to 120° (Table 11).

6.3. Variation of the wavelength

Fig. 13 presents the isotherms and the streamlines inside the cavity with $A = 5$. Various wavelength values were also studied with different values of α.

The influence of the non-uniform variation of the temperature on the vertical walls is established. The isotherms form cells on the hot and cold walls respectively. The number of these cells is equal to the number of the wavelength.

On the hot wall of the cavity, a thin thermal boundary layer was observed on these cells for all values of α studied. This phenomenon involves an increase in the heat transfer. The fluid motion generates several cells due to the increase in the volumetric flow for all wavelength values.

The flow is accelerated in the case ($k = 2$) and when α passes from 0.2 to 0.4. This causes the appearance of cells to the two symmetrical corners of the cavity. Table 12 gives the maximum values of the stream function with their position in (X, Y). The velocity of the cells increases when k varies periodically between the even and odd values. Another observation was made for a fixed Rayleigh number; when the maximum value of the stream function decreases, the value of the average Nusselt number increases.

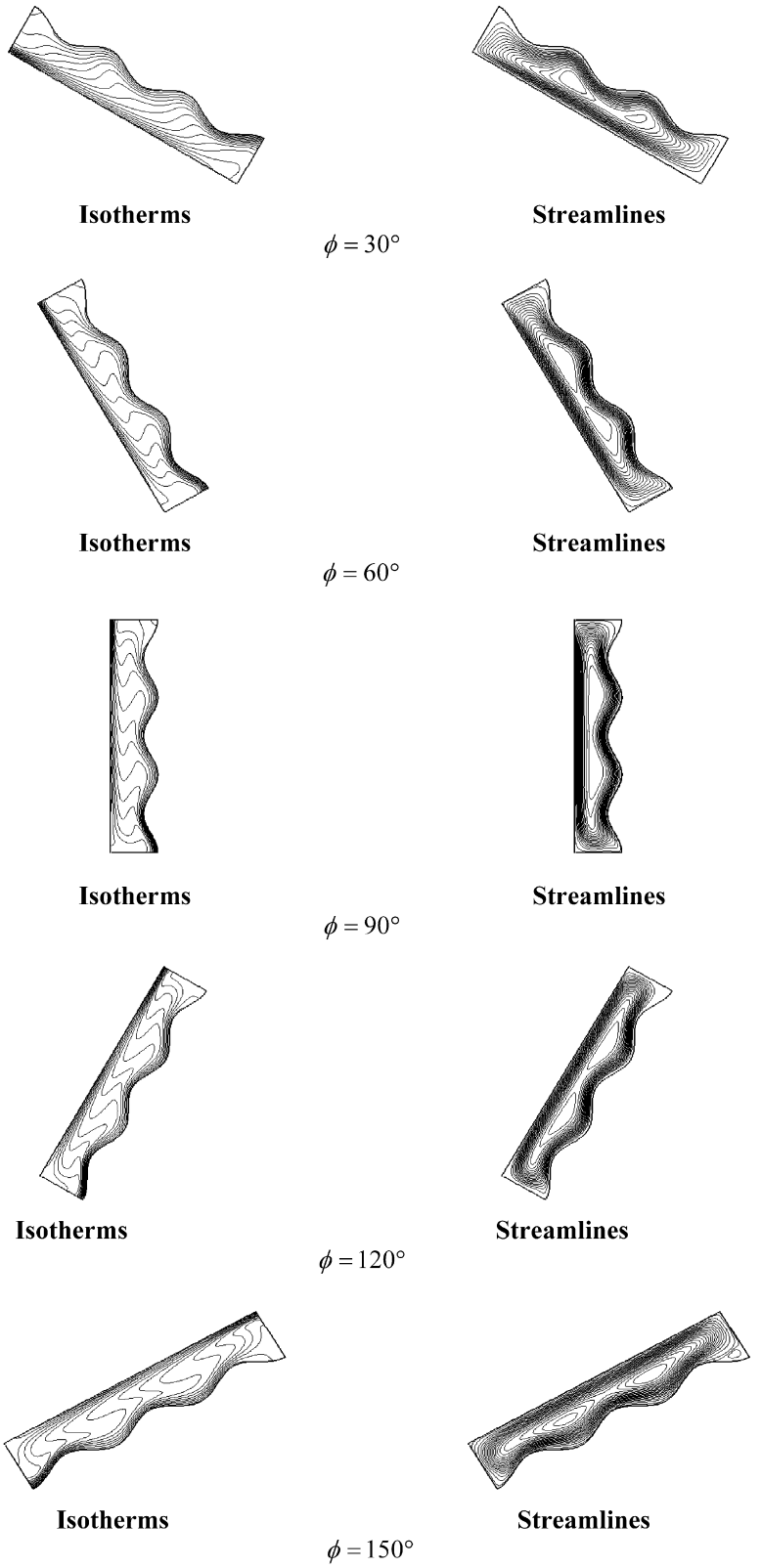

Fig. 12. Isotherms and streamlines for different inclination angle ($A = 5$).

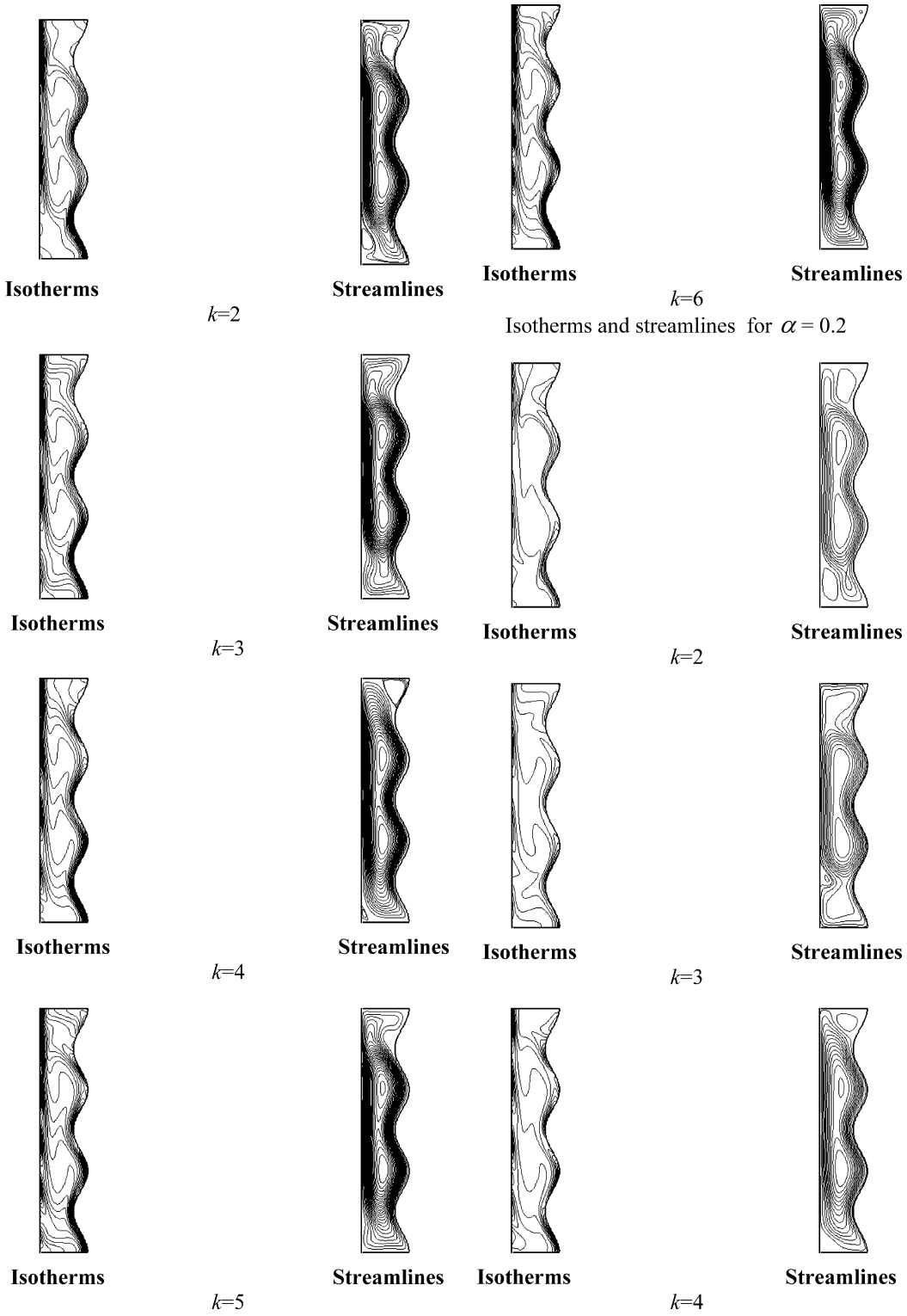

Fig. 13. Isotherms and streamlines for all k studied and all α ($A = 5$).

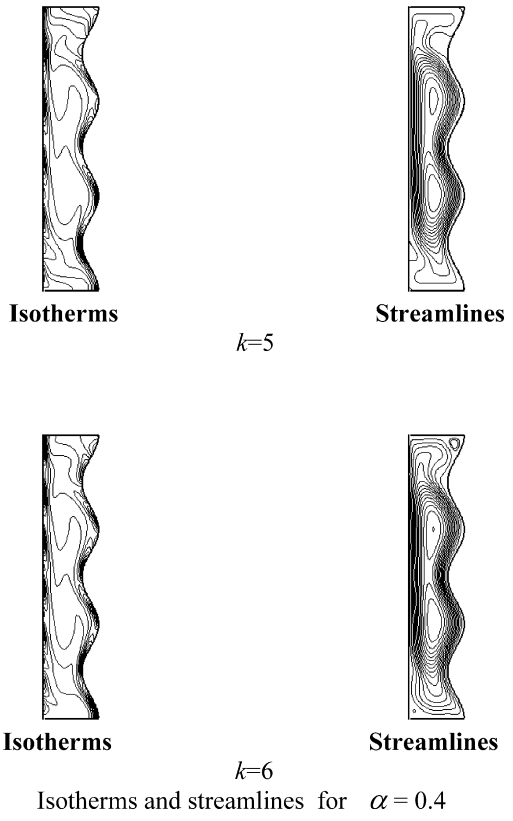

Fig. 13. (*continued*)

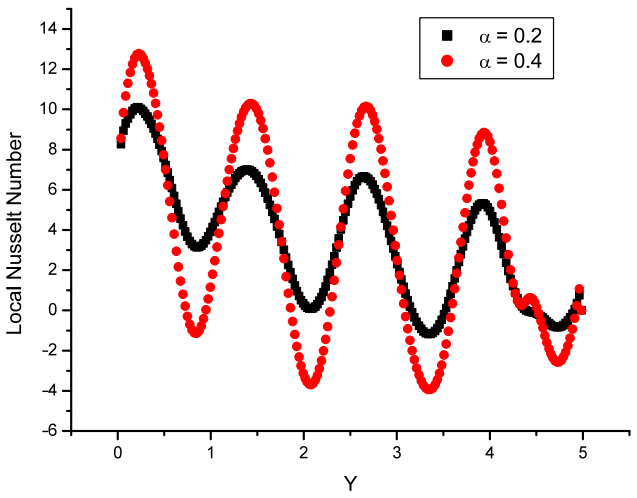

Fig. 14. Variation of the local Nusselt number along the hot wall ($A = 5$) and $k = 4$.

Table 12
Maximum value of the stream function for all values of α and k.

k	1	2	3	4	5
ψ_{Max} ($\alpha = 0.2$)	17.77	26.78	23.97	24.18	23.78
X	0.40	0.41	0.41	0.42	0.42
Y	1.84	1.97	2.06	1.98	2.07
ψ_{Max} ($\alpha = 0.4$)	15.20	29.85	24.03	25.22	24.68
X	0.34	0.39	0.45	0.38	0.41
Y	2.34	2.06	2.02	1.99	2.05

ψ_{Max} ($\alpha = 0$) = 24.66

The trend of the local Nusselt number curve follows the undulation of the temperature which has a sinusoidal form. The four peaks observed in the curve correspond well to the tightening of the thermal boundary layer along the hot wall. In addition the minimal points result from the relaxation of the thermal boundary layer (Fig. 14).

Table 13 includes all the values of the average Nusselt number for the studied cavities. For k equals to 2, a decrease of the thermal heat transfer is observed when α passes from 0.2 to 0.4 and this for all the studied cavities.

In fact, the geometry of the hot wall affects the value of average Nusselt number for all the studied wavelengths. It influences the shape of the curve of local Nusselt number for only one wavelength. For k different from 1, the trend of the curve of local Nusselt number corresponds to the distribution of the temperature.

7. Conclusion

The work presented in this paper concerns the study of the natural convection in the two-dimensional cavities. A simulation of the dynamic and thermal behaviour of the viscous and incompressible laminar flows was carried out. The modelling of this problem was expressed by the Navier–Stokes equations coupled with the equation of energy. Their resolution was made by the finite volume method. The SIMPLE algorithm is employed for the treatment of the coupling velocity and pressure. The grid of the geometries was validated with other publications. The aim of this work was to control the effect which

Table 13
Variation of the average Nusselt number for all the studied cavities.

A	k	1	2	3	4	5
3	$\overline{Nu}$ ($\alpha = 0.2$)	3.85	3.307	3.436	3.46	3.439
	$\overline{Nu}$ ($\alpha = 0.4$)	3.98	3.201	3.462	3.532	3.493
5	$\overline{Nu}$ ($\alpha = 0.2$)	3.72	3.289	3.41	3.30	3.42
	$\overline{Nu}$ ($\alpha = 0.4$)	3.88	3.195	3.43	3.50	3.46
7	$\overline{Nu}$ ($\alpha = 0.2$)	3.64	3.24	3.45	3.29	3.31
	$\overline{Nu}$ ($\alpha = 0.4$)	3.86	3.186	3.42	3.32	3.45
12	$\overline{Nu}$ ($\alpha = 0.2$)	3.17	2.88	3.14	2.943	2.989
	$\overline{Nu}$ ($\alpha = 0.4$)	3.44	2.85	3.40	3.17	3.39
15	$\overline{Nu}$ ($\alpha = 0.2$)	3.024	2.69	2.81	2.76	2.80
	$\overline{Nu}$ ($\alpha = 0.4$)	3.22	2.87	3.28	3.006	2.91

could have the flow and the heat transfer with the non-uniform distribution of the temperature on the vertical walls. In the first part of this paper, the study was carried out on regular cavities namely the square cavity.

For the sinusoidal distribution, several wavelengths were taken into account. The isotherms were affected by this distribution; however the intersection of the lines with the vertical walls causes a decrease in the cell size when the wavelength value increases.

The streamlines present a mono cellular flow pattern where small cells are superimposed in the central part of the cavity. The velocity of the cells increased when k varies periodically between the even and odd values. This causes the separation of the central cell into two. As for the heat transfer, it was increased for the odd wavelengths towards the growing direction of the α value. However it was noticed a decrease for the even wavelength values.

The second part of this study concerns the cavity with wavy hot wall. The same distributions of temperature were imposed. The inclination angle of the cavities was taken into account.

It induces an acceleration of the flow in the increasing direction of the angle. This causes the appearance of several small cells. Initially only one wavelength of the distribution of temperature was considered. The thickness of thermal boundary layer appears on the top of the undulations where an increase was noticed in the heat transfer. The curve of the local Nusselt number highlighted three peaks corresponding to the three tops of the hot wall. This confirms the analysis of the thermal boundary layer evolution made before.

Furthermore, a variation in the wavelength of the sinusoidal distribution was studied. It was noted that:

- The isothermal lines are affected by this distribution.
- The number of cells observed on the vertical walls is equal to the number of undulations.
- The trend of the local Nusselt number curve is sinusoidal and corresponds to the distribution of the temperature not to the geometry of the hot wall.
- The streamlines are influenced by the sinusoidal variation; the velocity of the cells involves separations.
- It was also noted that for a number of Rayleigh given, the value of average Nusselt number increases when the maximum value of the stream function decreases. The same remarks were established for cavities with aspect ratio higher than 1.
- The optimal distribution of temperature which reduces the heat transfer is the sinusoidal distribution with two wavelengths and α equal to 0.4.

Acknowledgements

The helpful comments of the reviewers are gratefully acknowledged by the authors.

References

[1] G. De Vahl Davis, Natural convection of air in a square cavity: a benchmark numerical solution, International Journal of Numerical Methods in Fluids 3 (1983) 249–264.
[2] I. Catton, Natural convection in enclosures, in: Proceedings of the Sixth International Heat Transfer Conference, vol. 6, 1978, pp. 13–31.
[3] S. Ostrach, Natural convection in enclosures, Advances in Heat Transfer 8 (1972) 161–227.
[4] K.T. Yang, Natural convection in enclosures, in: Handbook of Single Phase Convective Heat Transfer, Wiley, New York, 1987, pp. 13-1–13-51.
[5] A. Bejan, A. Anderson, Heat transfer through single and double vertical walls in natural convection: theory and experiments, International Journal of Heat and Mass Transfer (24) (1980) 1611–1620.
[6] J.N. Arnold, I. Catton, D.K. Edwards, Experimental investigation of natural convection in inclined rectangular regions of differing aspect ration, Journal of Heat Transfer 98 (1976) 67–71.
[7] H. Ozoe, K. Yamamoto, H. Sayama, S.W. Churchill, Natural circulation in an inclined rectangular channel heated on one side and cooled in opposing side, International Journal of Heat and Mass Transfer 17 (17) (1974) 1209–1217.
[8] K.G.T. Hollands, G.D. Raithby, Analysis of heat transfer by natural convection across vertical fluid layers, Journal of Heat Transfer 99 (2) (1973) 203–213.

[9] R.A. Kuyper, T.H.H. Vander Meen, C.J. Hoogendoorn, A.W.M. Henkes, Numerical study of laminar and turbulent natural convection in an inclined square cavity, International Journal of Heat and Mass Transfer 36 (11) (1993) 2899–2911.
[10] J.O. Wilkes, S.W. Churchill, The finite-difference computation of natural convection in a rectangular enclosure, American Institute of Chemical Engineers Journal 12 (1966) 161.
[11] H.N.S. Chu, S.W. Churchill, The development and testing of a numerical method for computation of laminar natural convection in enclosures, Computers & Chemical Engineering 1 (1977) 103.
[12] S.A. Korpela, Y. Lee, Multicellular natural convection in a vertical slot, Journal of Fluid Mechanics 126 (1983) 91.
[13] L.S. Yao, Natural convection along a vertical wavy surface, Journal of Heat Transfer 105 (1983) 465–468.
[14] C. Saidi, F. Legay, B. Pruent, Laminar flow past a sinusoidal cavity, International Journal of Heat and Mass Transfer 30 (1987) 649–660.
[15] L. Adjlout, O. Imine, A. Azzi, A. Belkadi, Laminar natural convection in an inclined cavity with a wavy wall, International Journal of Heat and Mass Transfer 45 (2002) 2141–2152.
[16] M. Belkadi, M. Aounallah, O. Imine, L. Adjlout, Y. Addad, Free convection in an inclined square cavity with partial partitions on a wavy hot wall, Progress in Computational Fluid Dynamics 6 (7) (2006) 428–434.
[17] B. Gilly, P. Bontoux, B. Roux, Influence of thermal wall conditions on the natural convection in a vertical rectangular differentially heated cavity, International Journal of Heat and Mass Transfer 24 (1981) 829–841.
[18] M. Bassey, O.G. Schmidt, Le séchage solaire en Afrique Compte rendu du colloque tenu à Dakar, Sénégal, du 21 au 24 juillet 1986.
[19] P. Chao, H. Ozoe, S.W. Churchill, Effect of a non-uniform surface temperature on laminar natural convection in a rectangular enclosure, Chemical Engineering Communications 9 (1–6) (1981) 245–254.
[20] V. Shukla, R. Murtugudde, V. Prasad, M. Cane, Natural convection in a horizontal cavity with a linear temperature variation on the top, in: 27th National Heat Transfer Conference, Mixed Convection Heat Transfer, Minneapolis, ASME HTD, vol. 163, pp. 1–8.
[21] Jian Li, D.B. Inghaam, I. Pop, Natural convection from a vertical flat plat with a surface temperature oscillation, International Journal of Heat and Mass Transfer 44 (2001) 2311–2322.
[22] S.V. Patankar, Numerical Heat Transfer and Fluid Flow, Series in Computational Methods in Mechanics and Thermal Sciences, McGraw–Hill Book Company, 1980.
[23] H.K. Versteeg, W. Malalasekera, An Introduction to Computational Fluid Dynamics, the Finite Volume Method, Longman Group Ltd., Malaysia, 1995.
[24] D. Amaresh, M.D. Kumar, Laminar natural convection in an inclined complicated cavity with spatially variable wall temperature, International Journal of Heat and Mass Transfer 48 (2005) 2986–3007.
[25] B.D. Thompson, F.C. Thames, F. Mastin, Automatic numerical generation of body-fitted curvilinear co-ordinate system, Journal of Computational Physics 15 (1974) 299–319.